



Comparison between Holocene and Marine Isotope Stage-11 sea-level histories

E.J. Rohling^{a,*}, K. Braun^b, K. Grant^a, M. Kucera^b, A.P. Roberts^a, M. Siddall^c, G. Trommer^b

^a School of Ocean and Earth Science, University of Southampton, National Oceanography Centre, Southampton SO14 3ZH, UK

^b Institute of Geosciences, University of Tübingen, Sigwartstrasse 10, 72076, Tübingen, Germany

^c Department of Earth Science, University of Bristol, Will's Memorial Building, Queen's Road, Bristol BS8 1RJ, UK

ARTICLE INFO

Article history:

Received 11 September 2009

Received in revised form 15 December 2009

Accepted 30 December 2009

Available online 25 January 2010

Editor: P. DeMenocal

Keywords:

sea level
interglacials
climate forcing

ABSTRACT

The exceptionally long interglacial warm period known as Marine Isotope Stage 11 (MIS-11; 428–397 ky ago vs. ky vs. kyr) is often considered as a potential analogue for future climate development in the absence of human influence. We use a new high-resolution sea-level record—a globally integrated ice-volume signal—to compare MIS-11 and the current interglacial (Holocene). It is found that sea-level rise into both interglacials started over similar timescales relative to the respective insolation increases, and progressed up to ~50 m at similar rates of 1.0–1.2 m per century. Subsequent weak insolation changes anomalously prolonged the MIS-11 deglaciation over more than 20 ky. The main sea-level highstand was achieved at the second MIS-11 insolation maximum, with a timing closely equivalent to that of the Holocene highstand compared to its single insolation maximum. Consequently, while MIS-11 was an exceptionally long period of interglacial warmth, its ice-volume minimum/sea-level highstand lasted less than 10 ky, which is similar to the duration of other major interglacials. Comparison of the ends of MIS-11 and the Holocene based on timings relative to their respective maxima in mean 21 June insolation at 65°N suggests that the end of Holocene conditions might have been expected 2.0–2.5 ky ago. Instead, interglacial conditions have continued, with CO₂, temperature, and sea level remaining high or increasing. This apparent discrepancy highlights the need to consider that: (a) comparisons may need to focus on other orbital control indices, in which case the discrepancy can vanish; and/or (b) the feedback mechanisms that dominate the planetary energy balance may have become decoupled from insolation during the past 2 millennia.

© 2010 Elsevier B.V. All rights reserved.

1. Introduction

MIS-11 is often considered as a potential analogue for future climate development because of relatively similar orbital climate forcing (e.g., Droxler and Farrell, 2000; Loutre and Berger, 2000, 2003; McManus et al., 2003; Masson-Delmotte et al., 2006; Dickson et al., 2009). However, there is an obvious difference in that the current interglacial (Holocene) spans a single insolation maximum (summer, 65°N), while MIS-11 spanned two (weak) astronomical precession-driven insolation maxima separated by a minor minimum (due to coincidence of a minimum in 400-ky orbital eccentricity with a maximum in the Earth's axial tilt (Laskar et al., 2004)). Important evidence for the anomalously long duration of MIS-11 across two successive insolation maxima comes from atmospheric CH₄, CO₂ and temperature records from Antarctic ice cores, whereas all 'typical' interglacials since that time terminated after one insolation maximum (EPICA Community Members, 2004; Siegenthaler et al., 2005; Jouzel et al., 2007; Loulergue et al., 2008). Antarctic temperature and CO₂ did not evidently respond to the weak insolation minimum within MIS-

11, but other data suggest a brief (and commonly mild) relapse to more glacial-style conditions (Loulergue et al., 2008; Dickson et al., 2009). A long period of interglacial warmth (with a brief relapse within MIS-11) is also evident from high-resolution temperate pollen records (Tzedakis, 2009).

Until recently, understanding ice-volume history through MIS-11 has been impaired by a lack of continuous and highly resolved time-series of sea-level change. For many years, deep-sea benthic foraminiferal stable oxygen isotopes ($\delta^{18}\text{O}$) provided the best continuous records, but they suffer from large potential complications associated with unconstrained deep-sea temperature changes. Qualitatively, these records suggest that the MIS-11 sea-level highstand occurred during the second (larger) MIS-11 insolation maximum, with a similar magnitude as the current interglacial (Holocene) highstand (McManus et al., 1999, 2003; Lisiecki and Raymo, 2005). For the first time, we here use a recently published, independent, continuous, and highly resolved relative sea-level (RSL) record through MIS-11 and the Holocene from the Red Sea method (Rohling et al., 2009).

2. Materials and methods

The Red Sea method exploits changes in the residence-time of water in the highly evaporative Red Sea that result from sea-level

* Corresponding author.

E-mail address: e.rohling@noc.soton.ac.uk (E.J. Rohling).

Table 1
U/Th based ages of coral and speleothem samples of past interglacials.

Coral and speleothem data					Continuous sea-level record after age adjustment		
Marine Isotope Stage	Narrowly defined age (yr)	Narrowly defined uncertainty range (yr)	Broadly defined age (yr)	Broadly defined uncertainty range (yr)	Age (yr)	Narrowly defined uncertainty range (yr)	Broadly defined uncertainty range (incl. early and late spikes; yr)
1	3500	±3500	3500	±3500	3550	±3550	−4350/+4350
5e	120000	±4000	124500	±7500	123250	±4550	−6750/+5550
7a	197000	±3000	195500	±7500	196600	±2000	−2000/+2000
7e	237000	±1000	239400	±11400	237300	±600	−600/+600
9c	321000	±8000	321000	±8000	325950	±1450	−1450/+1450
11	404000	±6000	404000	±6000	402050	±2700	−2700/+4650
13	480000	±7000	480000	±7000	484300	±700	−700/+700

The 'narrow' definition is as compiled in Siddall et al. (2009). The 'broad' definition is as compiled in Siddall et al. (2006) and Rohling et al. (2009). These values are compared with sea-level data used here after the chronological adjustment discussed in Materials and methods. Interglacials in the continuous record of Rohling et al. (2009) are measured on the basis of upcrossings through -10 m.

imposed changes in the dimensions of the very shallow (137 m) Strait of Bab-el-Mandab, which is the only natural connection between the Red Sea and the open ocean (Winter et al., 1983; Locke and Thunell, 1988; Thunell et al., 1988; Rohling, 1994; Rohling et al., 1998; Siddall et al., 2002, 2003, 2004). The concentration effect causes high salinities and heavy $\delta^{18}\text{O}$ in the Red Sea with falling sea level, and is constrained as a function of sea level by hydraulic control calculations for the Strait (Rohling et al., 1998; Siddall et al., 2002, 2003, 2004). The sensitivity of $\delta^{18}\text{O}$ to sea-level change is then applied to translate planktonic foraminiferal $\delta^{18}\text{O}$ records from central Red Sea sediment cores into records of relative sea-level change. The theoretical confidence limit of ± 6 m (1σ) (Siddall et al., 2003, 2004) is confirmed by practical reproducibility margins of ± 6.5 m (1σ) (Rohling et al., 2009). Results from the Siddall et al. (2003, 2004) calculations were corroborated using an independent (numerical) quantification approach (Biton et al., 2008), as well as by empirical scaling of independent Red Sea records to coral-reef sea-level data (Arz et al., 2007).

Response times of $\delta^{18}\text{O}$ in the Red Sea surface-water system to sea-level change are less than a century (Siddall et al., 2004; Biton et al., 2008; Rohling et al., 2008a). The method produces excellent within-basin reproducibility based on analyses by different teams in different labs, using different cores and different materials (Siddall et al., 2003, 2008; Arz et al., 2007; Rohling et al., 2008a, 2009). The various quantification methods include isostatic components (Siddall et al., 2004; Biton et al., 2008; see also Rohling et al., 2008b), and tectonic influences were empirically constrained (Rohling et al., 1998; Siddall et al., 2003, 2004). Agreement with coral/speleothem markers from around the world demonstrates that Red-Sea-based records closely reflect global sea-level change (Siddall et al., 2003, 2004, 2006, 2008; Rohling et al., 2008a, 2009; Dutton et al., 2009; Thomas et al., 2009; Kopp et al., 2009).

The record used here is the latest composite sea-level record from the Red Sea method (Rohling et al., 2009). It combines data for different carbonate phases (foraminiferal carbonate and bulk sediment) from three central Red Sea cores, namely KL11, MD92-1017, and KL09. Core KL11 spans the interval 0–360 ka, MD92-1017 the interval 0–470 ka, and KL09 the interval 0–520 ka. Reproducibility of the sea-level signals between the various datasets is ± 6.5 m (1σ) throughout the record, and the overall mean temporal resolution of the composite is ~ 250 yr.

Rohling et al. (2009) constrained the chronology of the sea-level record by graphic correlation to the EPICA Dome C ice-core Antarctic Temperature anomaly record of Jouzel et al. (2007), using the EDC3 time scale (Parrenin et al., 2007). Parrenin et al. (2007) noted that the EDC3 chronology seems to be systematically offset from the stacked global deep-sea benthic oxygen isotope record of Lisiecki and Raymo (2005), which contains a considerable ice-volume component. Rohling et al. (2009) supported this observation, noting that straightforward use of the EDC3 chronology for sea level would imply a systematic offset from radiometric U–Th ages of coral and

speleothem sea-level benchmarks. The offset was ascribed to a lagged response of ice volume/sea level to temperature change, resulting from inertia in the ice response that makes it react to heating/cooling over a longer, integrated millennial-scale period rather than to instantaneous temperature.

To convert the sea-level record to a U–Th equivalent chronology, we shift it to systematically 4 ky younger values, based on the offset between the EDC3 age and the radiometric age from fossil corals for the mid-point of the last deglaciation. Only in the Holocene do we deviate from this simple -4 ky shift; there, the chronology of the sea-level record is linearly scaled from 'EDC3–4ky' at the end of the last deglaciation, to 0 ka at the top. The resultant sea-level chronology is within 500 yr of radiocarbon constraints in the Holocene (Siddall et al., 2003), and within 1.5% of U–Th datings as previously compiled for all major interglacials of the past 500 kyr (Siddall et al., 2006,

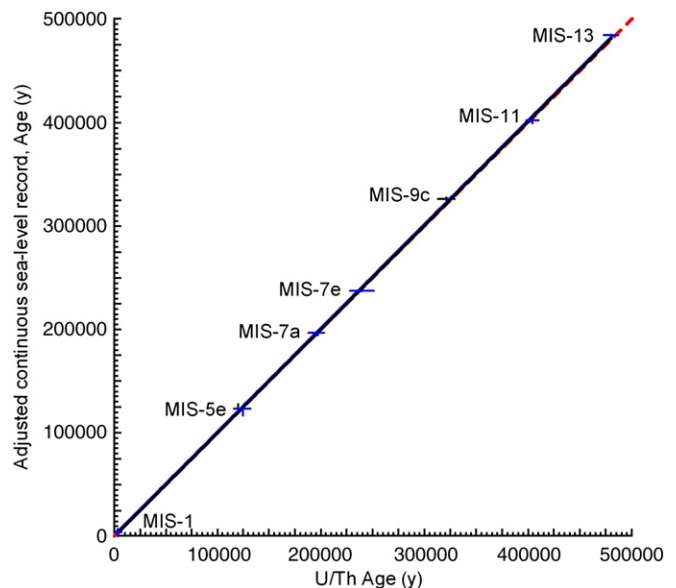


Fig. 1. Comparison of the chronology of the continuous sea-level record (Rohling et al., 2009) after adjustment as described in Materials and methods. Data are as listed in Table 1. One scenario (black) uses narrowly-defined U–Th age ranges (Siddall et al., 2009) compared with intervals where the continuous sea-level record (Rohling et al., 2009) exceeds -10 m excluding early and late individual spikes. A second scenario (blue) uses broadly defined U–Th age ranges (Siddall et al., 2006; Rohling et al., 2009) compared with intervals where the continuous sea-level record (Rohling et al., 2009) exceeds -10 m including early and late individual spikes. Black and blue lines are linear regressions through the two scenarios; both have $r^2 > 0.998$, and a slope of 1.0 (within a margin of 0.004). The mid-point age difference is typically within $\pm 1.5\%$ (Table 1), and both linear regressions are indistinct from the equal-age isoline (red, dashed).

2009; Rohling et al. 2009) (Table 1, Fig. 1). The adjustment also brings the sea-level chronology into close agreement with that of the Lisiecki and Raymo (2005) benthic oxygen isotope record. There are two major advantages to our ‘anchoring’ (on orbital scales) of the sea-level chronology to radiometrically dated sea-level benchmarks. First, it allows reliable plotting of sea level alongside records of the various orbital insolation solutions. Second, it makes the sea-level chronology independent of adjustments/uncertainty in the ice-core chronologies.

We show the ice-core data using the EDC3 chronology (Parrenin et al., 2007). For glacial terminations 2 (T2), T3, and T4, Kawamura et al. (2007) reconstructed ages for Dome Fuji that are older, namely about EDC3 + 2 kyr, EDC3 + 1 kyr, and EDC3 + 3 kyr, respectively. Given that no Dome Fuji ages have (yet) been published for T5, we tentatively use the T4 result of Kawamura et al. (2007) to infer a + 3 kyr age uncertainty for T5 in our plots of the Antarctic ice-core data. As stated above, the U–Th anchored sea-level chronology is not affected by that uncertainty.

We also present planktonic foraminiferal data for the Holocene and MIS-11 from the same samples as the sea-level data (Fig. 2). This gives us local central Red Sea control on peak interglacial intervals. If the Holocene and MIS-11 are properly ‘aligned’ using the sea-level signal, then peak interglacial conditions in the same samples as indicated by the faunas should also be reasonably well aligned; in other words, the faunas provide an internal validation criterion for any ‘alignment’. We do not use the faunas to compare with peak interglacial conditions from other data in other records because that would require assumptions about extra-regional synchronicity and comparability between different types of proxy data, which we explicitly wish to avoid. Finally, we present magnetic susceptibility data—also from the same samples as the sea-level reconstruction—which in the Red Sea record has been found to reflect wind-blown dust (hematite) input, and which was found to be systematically high

during glacials and low during interglacials, probably due to a combination of source availability (soil moisture?) and wind strength/direction (Rohling et al., 2008b).

3. Comparison between MIS-11 and the Holocene

The sea-level record of Rohling et al. (2009) represents a continuous time-series that is based on a uniform technique applied to multiple sedimentary archives that include both MIS-11 and the Holocene. It places the MIS-11 highstand at a similar (within uncertainty) level as the Holocene highstand. This contradicts other, time-slice specific suggestions of potentially high MIS-11 sea levels (e.g., Droxler and Farrell, 2000; Hearty and Olsen, 2007; and references therein), but confirms temporally continuous global deep-sea benthic $\delta^{18}\text{O}$ records (McManus et al., 1999, 2003; Lisiecki and Raymo, 2005; Dickson et al., 2009). If any rapid fluctuations to + 10 or even + 20 m had occurred within MIS-11, then these would at ‘typical’ fast interglacial rates of rise of up to 2 m/century and lowering of ~1 m/century (Rohling et al., 2008a) have spanned 1500 to 3000 yr, which would not go undetected in the Red Sea record. Given that there is no indication of this, the Red Sea record strongly supports the MIS-11 sea-level review of Bowen (2009), which also places MIS-11 sea level within uncertainties at the present-day level.

Our record of sea-level changes is a globally integrated signal of ice-volume change that avoids potential bias associated with region-specific climate records, and its chronology is ‘anchored’ to radiometric ages of sea-level benchmarks for all major interglacials considered (Table 1, Fig. 1). It therefore offers strong validation regarding the temporal (insolation-based) ‘alignment’ for comparison between the onset of the last deglaciation (Termination 1, T1) and that into MIS-11 (T5), as shown in Fig. 3. This alignment is similar to that suggested previously (EPICA Community Members, 2004;

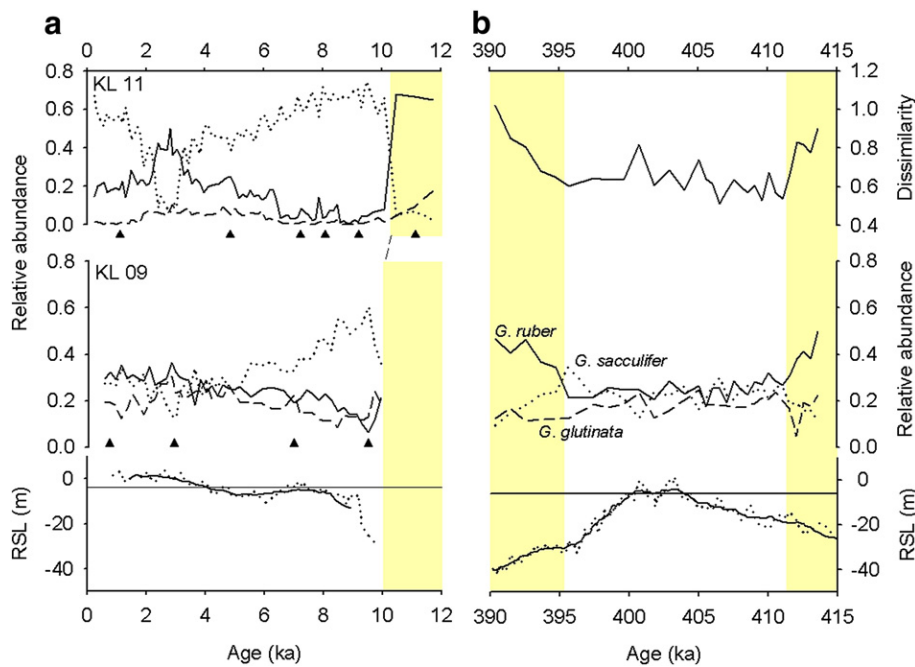


Fig. 2. Comparison of planktonic foraminiferal assemblages between the Holocene and MIS-11 with the Red Sea relative sea-level (RSL) record (Rohling et al., 2009). a. Relative abundances of the three dominant planktonic foraminiferal species throughout the Holocene in cores GeoTü KL11 (Schmelzer 1998) and GeoTü KL09 (Siccha et al., 2009), which highlights development of the modern-type fauna at ~10.5 ka when sea level stood at ~25 m below the present day (the shaded area indicates glacial-type fauna in KL11 and interval of indurated sediment section, which is typical for glacial conditions in the Red Sea, in KL09); triangles indicate the positions of calibrated AMS ^{14}C ages on which the age model for the Holocene in both cores is based (Schmelzer, 1998; Siccha et al., 2009). b. Abundances of the same species as in (a) across the MIS-11 sea-level highstand from GeoTü KL09 together with their calculated maximum dissimilarity to the Holocene faunas from the same core. The faunal counts for MIS-11 were produced using the same methods as in Siccha et al. (2009). Glacial-like faunas before and after the MIS11 sea-level highstand are highlighted in yellow. Comparison with the RSL record indicates that Holocene-like faunas existed during MIS-11 when sea level stood higher than roughly – 25 m.

Broecker and Stocker, 2006), and it closely aligns the glacial maxima before T1 and T5. Our records reveal that the MIS-11 highstand was achieved only in association with the second MIS-11 insolation peak (Fig. 3d). The initial phases of deglaciation (up to -50 m) for T5 and T1 not only had similar timings relative to the preceding insolation minima, but they also had similar mean rates of change, with a 50–60 m rise in 5 kyr, or 1.0–1.2 m per century (Fig. 3d). During T5, however, sea level then remained at around -50 m for almost 4 kyr as insolation decreased from the first (minor) MIS-11 maximum. This was followed by a slow (~ 0.3 m per century) sea-level rise over 16 kyr up to the MIS-11 highstand (Fig. 3d).

Our observation that the Holocene interglacial ice-volume minimum is best compared with the latter phase of MIS-11 is supported by Holocene(-like) planktonic foraminiferal assemblages—dominated by *Globigerinoides sacculifer* and *Globigerinoides ruber* (with *Globigerinita glutinata*)—in the same samples as the highstand phase (Figs. 2, 3d). Also in the same sample series, the interglacial wind-blown dust minimum occurs at around the highstand period, following decreasing values through the first insolation maximum and a brief peak that predates the highstand phase (Fig. 3c).

To facilitate comparison of ice-volume signals through the highstands, we align our records using the second (larger) insolation

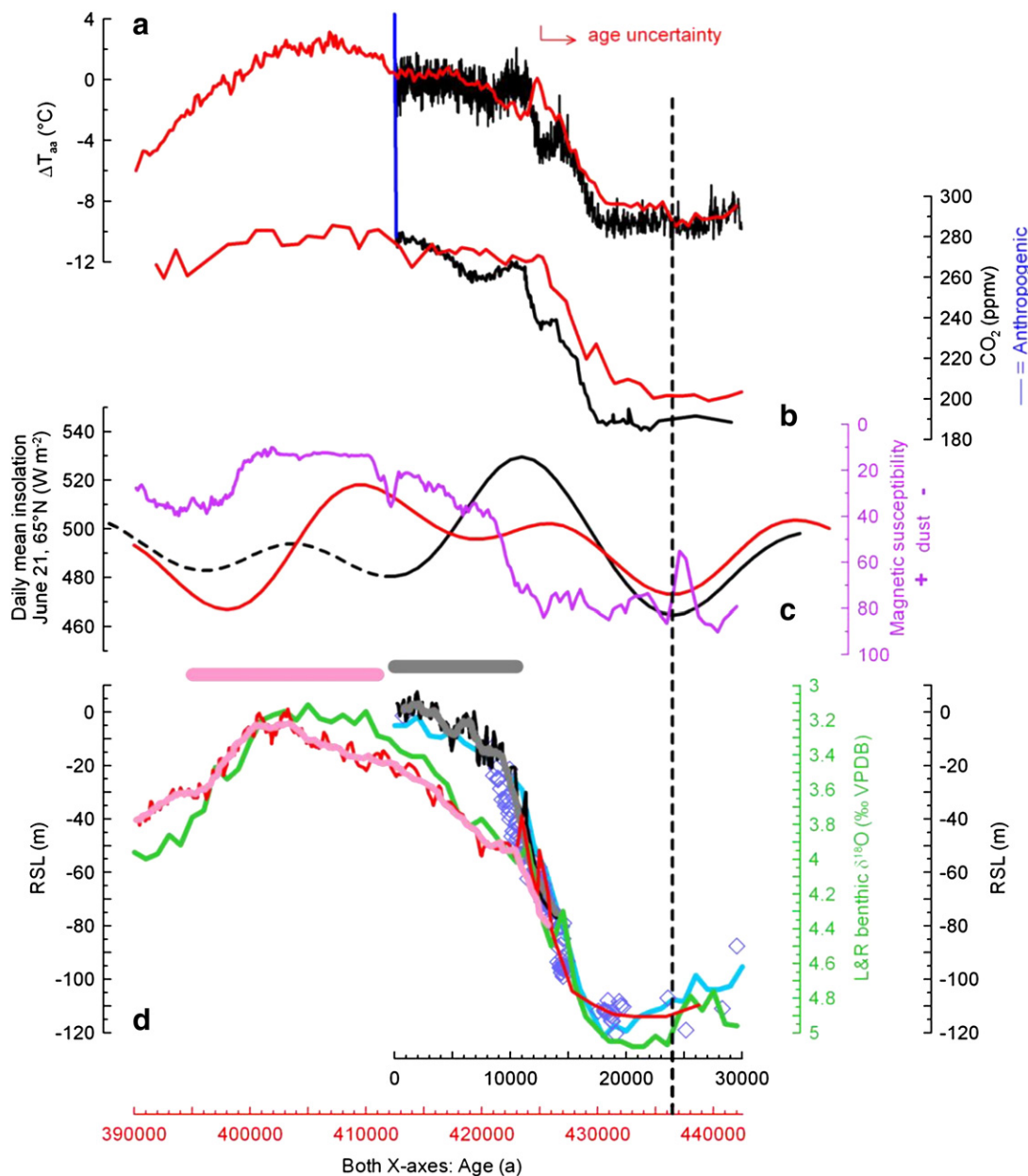


Fig. 3. Comparison of signals through MIS-11 (red) and the Holocene (black), as aligned (vertical dashed line) using the insolation minimum before the deglaciation. a. Antarctic ice-core temperature anomaly relative to the mean of the last 1000 yr (ΔT_{aa}) (Jouzel et al., 2007). b. Antarctic ice-core CO_2 concentrations (Siegenthaler et al., 2005). The blue line—which is virtually vertical on these timescales—represents the anthropogenic CO_2 increase over the last century to about 390 ppmv today. c. Mean insolation for 21 June at 65°N (Laskar et al., 2004), along with a (purple) magnetic susceptibility based record of wind-blown dust concentration in the central Red Sea (Rohling et al., 2008b). d. Relative sea-level (RSL) record for MIS-11 (red, and long-term average in pink) and the Holocene (black, long-term average in grey, and coral-based values in blue diamonds) (Rohling et al., 2009). Heavy green (MIS-11) and blue (Holocene) lines are records for the same intervals from the global benthic $\delta^{18}\text{O}$ stacked record (Lisiecki and Raymo, 2005). Thick horizontal bars indicate intervals with Holocene(-like) planktonic foraminiferal fauna in MIS-11 (pink) and the Holocene (grey) in the central Red Sea (see Fig. 2). The ΔT_{aa} and CO_2 records are presented using the EPICA Dome C 3 (EDC3) timescale (Parrenin et al., 2007), and a +3 kyr age uncertainty is indicated for the T5 date, based on the result for T4 from Kawamura et al. (2007). All corals are plotted using their original U–Th ages. Red Sea data are shown on the chronology discussed in this paper.

maximum of MIS-11 and the single Holocene insolation maximum (Fig. 4). This alignment is similar to that advocated previously by Loutre and Berger (2000, 2003), Crucifix and Berger (2006), and Ruddiman (2005, 2006). With this alignment, Holocene(-like) foraminiferal faunas were clearly established in the Red Sea with similar timings in both interglacials, when RSL rose above about -25 m. This alignment also reveals that the two highstands are similar within the intervals between 2 and 8.5 kyr after the insolation maxima (Fig. 4c,d). Glaciation (sea-level fall) commenced ~ 8.5 kyr after the MIS-11 insolation maximum, and Holocene-like fauna disappeared in MIS-11 when RSL dropped back below about -25 m at around 395 ka (Figs. 2, 4c,d). In the faunal data, peak interglacial conditions start at the same time, but last longer than in the wind-blown dust record; the dust record suggests that peak interglacial conditions (i.e., the dust minimum) had already ended at around

400 ka (Fig. 3c). Despite reasonably similar insolation histories, no glacial inception is apparent since the Holocene insolation maximum; sea level remains high (Fig. 4d). The CO_2 and ΔT_{aa} records also declined following a ~ 9 -kyr high after the final MIS-11 insolation maximum. In contrast, they stayed high (ΔT_{aa}) or even rose (CO_2) during the last 2 to 2.5 kyr of the Holocene (i.e., more than 9 kyr since the Holocene insolation maximum) (Fig. 4a,b). Note that use of a $+3$ kyr age correction in the EDC3 chronology of the ice-core ΔT_{aa} and CO_2 records for T5 (based on the age shift for T4; Kawamura et al., 2007) would only accentuate the discrepancy between dropping MIS-11 values and rising/stable Holocene values (Figs. 3–6).

The double insolation peak clearly makes MIS-11 different from ‘normal’ one-maximum interglacials. Deglaciation started with a similar timing relative to orbital insolation for both MIS-11 and the Holocene. However, subsequent weak insolation changes prolonged

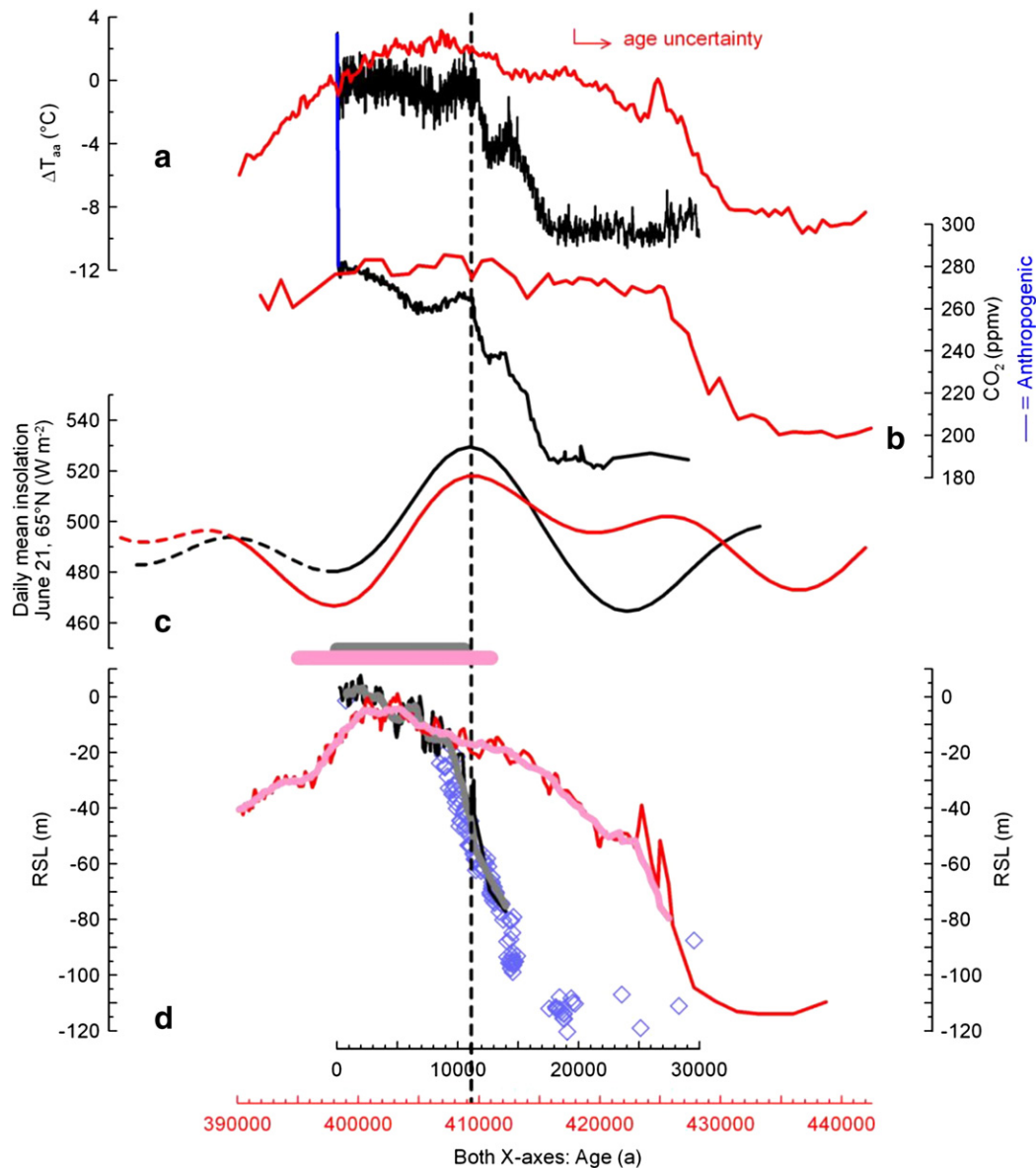


Fig. 4. Same as Fig. 3, but now aligned (vertical dashed line) using the peak insolation maximum. a. Antarctic ice-core temperature anomaly relative to the mean of the last 1000 yr (ΔT_{aa}) (Jouzel et al., 2007). b. Antarctic ice-core CO_2 concentrations (Siegenthaler et al., 2005). c. Mean insolation for 21 June at 65°N (Laskar et al., 2004). d. Relative sea-level (RSL) record for MIS-11 (red, and long-term average in pink) and the Holocene (black, long-term average in grey, and coral-based values in blue diamonds) (Rohling et al., 2009). Thick horizontal bars indicate intervals with Holocene(-like) planktonic foraminiferal fauna in MIS-11 (pink) and the Holocene (grey) in the central Red Sea. Chronologies are as in Fig. 1.

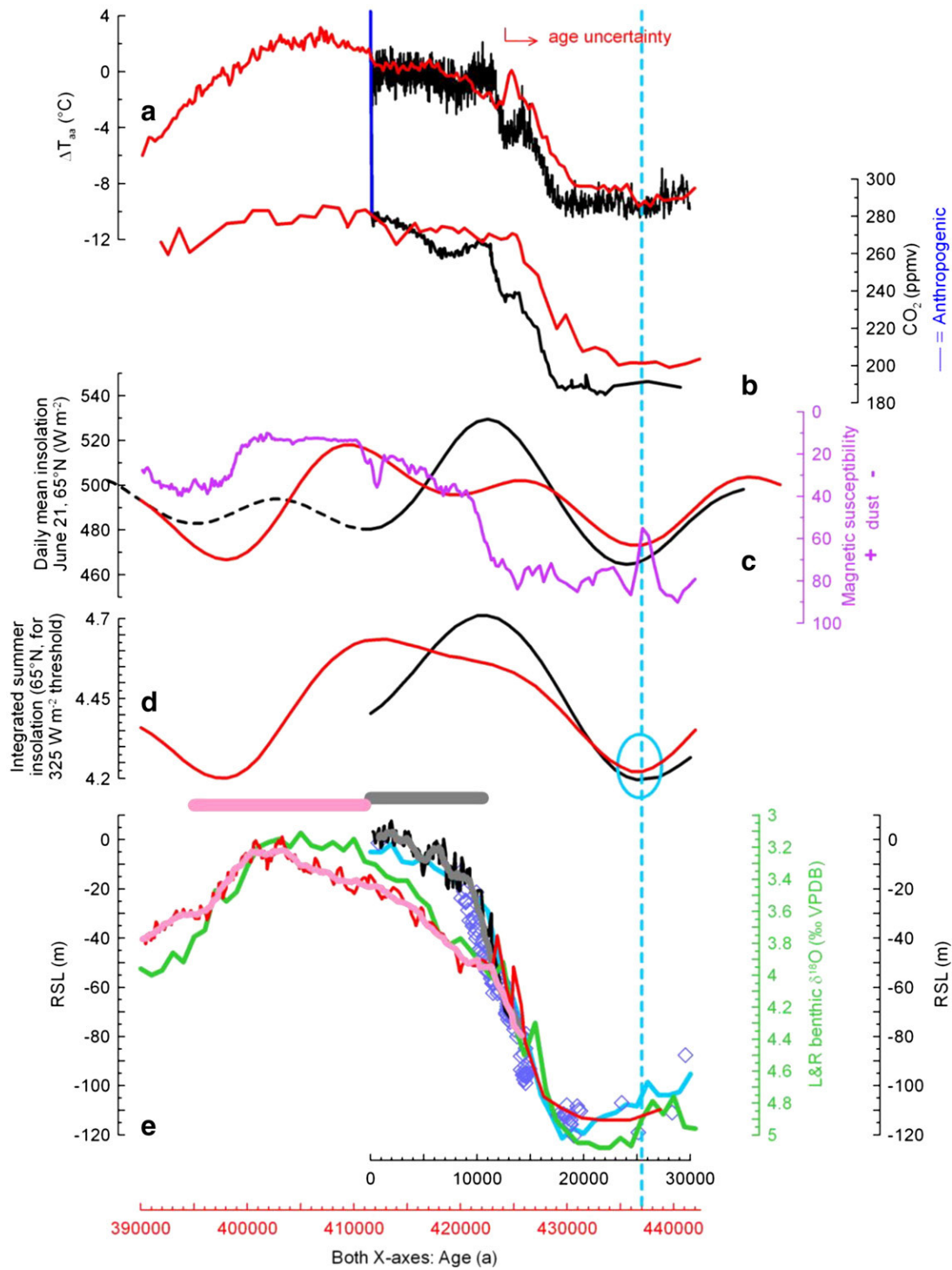


Fig. 5. The same plotted parameters as in Fig. 3, but using the integrated summer energy at 65°N for days with insolation above a threshold of 325 W m^{-2} (Huy325; Huybers, 2006) as shown in (d) to portray an alternative insolation alignment (see Discussion and conclusions). Panels a–c are as in Fig. 3a–c. New panel d is the Huy325 record. Panel e is as in Fig. 3d.

the MIS-11 deglaciation over an anomalously long period of time. First, a weak insolation minimum stabilized ice-volume. Then, slow ($0.3 \text{ m per century}$ sea-level equivalent) ice-volume reduction led to the final MIS-11 sea-level highstand, associated with the second insolation maximum. We find that, although MIS-11 marks an extended (25–30 kyr) period of warmth, the first 15–20 kyr of MIS-11 occurred as part of an extended deglaciation, while the actual interglacial ice-volume/sea-level highstand lasted less than 10 kyr, which is similar to that of other major interglacials in the past half million years.

4. Discussion and conclusions

We demonstrate that the Holocene sea-level history is best compared with the inception of MIS-11 and then with the highstand over the first 8.5 kyr after the second MIS-11 insolation maximum. Differences between climatic developments through MIS-11 and the Holocene might be ascribed to a ‘memory’ in the climate system (especially the ice sheets) that causes different time-integrated responses through the double insolation peak of MIS-11 relative to the single insolation peak of the Holocene. From that point of view,

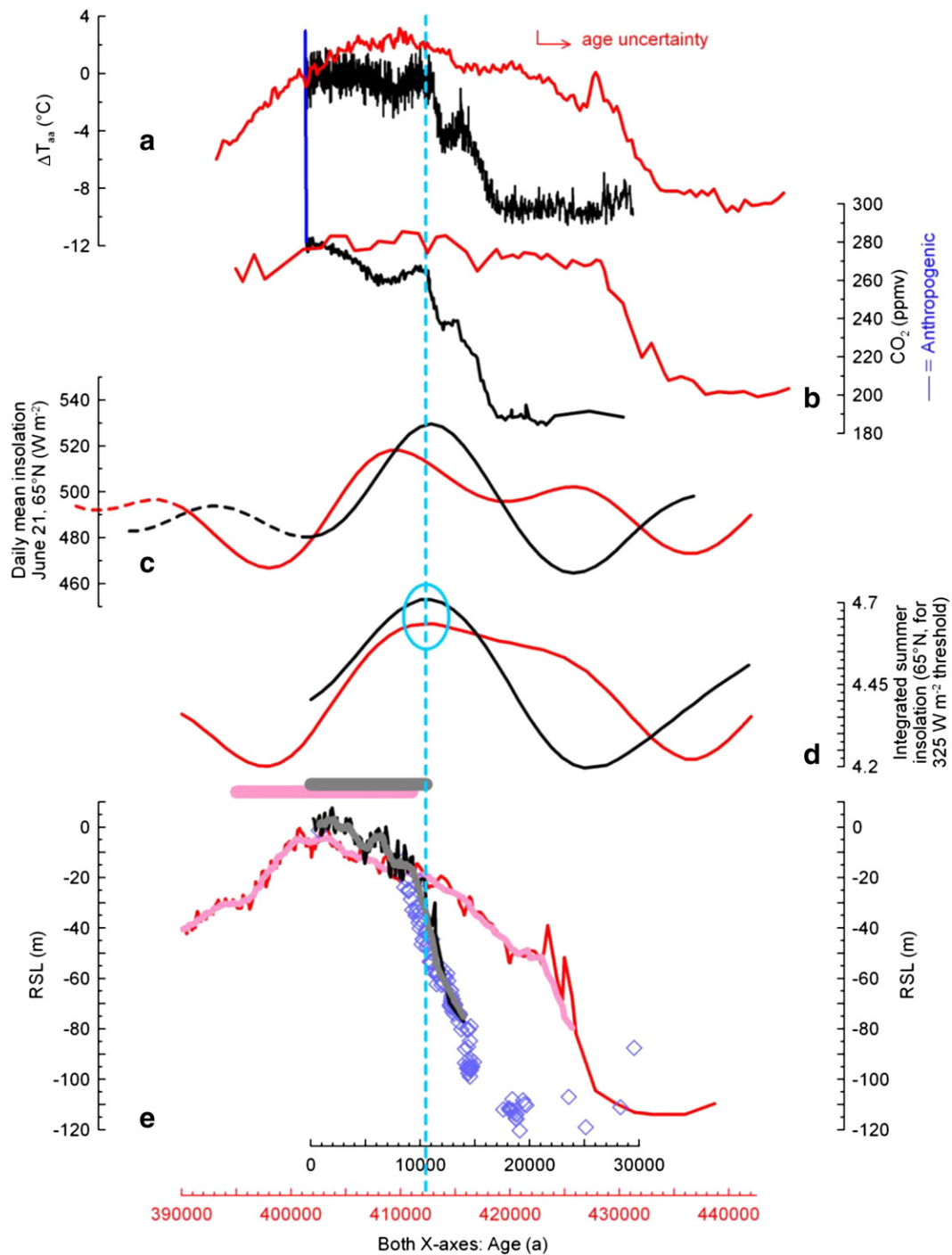


Fig. 6. The same plotted parameters as in Fig. 4, but using the Huy325 record (d) to portray an alternative insolation alignment (see Discussion and conclusions). Panels a–c are as in Fig. 4a–c. Panel d is the Huy325 record. Panel e is as in Fig. 4d.

the search for a direct analogue of the Holocene should be diverted to low-eccentricity interglacials associated with a single insolation maximum. This draws attention to MIS-19 (~780 ka), for which greenhouse gas concentrations can still be derived from Antarctic ice cores (Loulergue et al., 2008), although sea-level data similar to that used here for MIS-11 and the Holocene would require new, deep (Integrated Ocean Drilling Project) drilling in the central Red Sea. Recent comparisons of CO_2 and CH_4 trends through MIS-19 with those of the Holocene, in the absence of sea-level constraints, have been used to suggest that the Holocene should have terminated already (Kutzbach et al., 2009), although opinions remain divided (Tzedakis, 2009).

Regardless of whether developments toward the MIS-11 highstand can be used as an analogue for the Holocene or for future climate developments, the highstand and the insolation decrease marking its end are similar to those for the Holocene (Fig. 4c,d). Despite this similarity, and although the ice sheets during MIS-11 were exposed for much longer to generally increased insolation, our comparison in Fig. 4 suggests that the MIS-11 sea-level highstand ended 2.0–2.5 kyr sooner than the Holocene highstand (relative to the respective maxima of mean insolation for 21 June at 65°N).

On the one hand, the apparent 2.0–2.5 kyr discrepancy may suggest that—instead of mean insolation for 21 June at 65°N (Laskar et al., 2004) (Figs. 3c, 4c)—other orbital controls should be considered

(e.g., Huybers, 2006). The same alignments from Figs. 3 and 4 are shown in Figs. 5 and 6, but based on the record of integrated summer energy at 65°N for months with insolation above a threshold of 325 Wm⁻² (i.e., temperature above ~0°C), which is a leading alternative hypothesis for explaining the timing of Pleistocene glacial cycles, with a stronger obliquity influence (Huybers, 2006). The alignment based on this record (hereafter referred to as Huy325) for the onset of deglaciation (Fig. 5) is closely similar to that shown in Fig. 3. In contrast to Fig. 4, however, the alignment using Huy325 in Fig. 6 suggests that the Holocene sea-level highstand has not 'outlived' the MIS-11 highstand, and that modern sea level instead may remain high for another 2 kyr. Use of yet another orbital control index, namely the Milankovitch (1941) caloric summer half-year index (which also has added weight for obliquity relative to the June 21, 65°N insolation record) still places the best MIS-11 insolation analogue to the present near the precession-dominated insolation minimum of ~398 ka (Ruddiman, 2007) (as in Fig. 4). Clearly, questions remain as to the nature of the most applicable index for orbital insolation control. More profoundly, we question whether it is correct to expect that one specific index for orbital control would apply equally to deglaciation and glacial inception. Perhaps, for example, deglaciation is controlled by integrated summer energy, and glacial inception by instantaneous insolation values?

Finally, the alignment shown in Fig. 4 (which is similar to that of Ruddiman, 2005, 2007) exemplifies a completely different, more controversial (Spahni et al., 2005; Siegenthaler et al., 2005), possibility. It has been argued that variability in the planetary energy balance during Pleistocene glacial cycles was dominated by greenhouse gas and albedo related feedback mechanisms, and that the role of insolation was limited to only triggering the feedback responses (Hansen et al., 2008). Hence, the apparently anomalous climate trends of the most recent 2.0–2.5 millennia should also be investigated in terms of changes in these feedback responses due to processes other than insolation, including controversial suggestions concerning man's long-term impacts from deforestation and CH₄ and CO₂ emissions (Ruddiman, 2003, 2005, 2006, 2007; Hansen et al., 2008). There is support from modelling studies that the relatively minor early anthropogenic influences may have been sufficient to delay glacial inception (Vavrus et al., 2008; Kutzbach et al., 2009).

Targeted new research is needed—both into alternative orbital controls, and into the potentially long history of anthropogenic impacts on the main climate feedback parameters—before conclusive statements can be made about current climate developments based on the end of MIS-11.

Acknowledgements

This study contributes to UK Natural Environment Research Council (NERC) projects NE/C003152/1, NE/E01531X/1, NE/G015945/1 and NE/H004424/1, and German Science Foundation (DFG) projects He 697/17; Ku 2259/3. MS acknowledges support from an RCUK fellowship from the University of Bristol. We thank Peter deMenocal, Bill Ruddiman, Chronis Tzedakis and an anonymous reviewer for detailed comments and suggestions. Ice-core data are from the IGBP PAGES/World Data Center for Paleoclimatology. The sea-level data are available at <http://www.soes.soton.ac.uk/staff/ejr/ejrhome.htm>.

References

- Arz, H.W., Lamy, F., Ganopolski, A., Nowaczyk, N., Pätzold, J., 2007. Dominant Northern Hemisphere climate control over millennial-scale glacial sea-level variability. *Quat. Sci. Rev.* 26, 312–321.
- Biton, E., Gildor, H., Peltier, W.R., 2008. Relative sea level reduction at the Red Sea during the Last Glacial Maximum. *Paleoceanography* 23, PA1214. doi:10.1029/2007PA001431.
- Bowen, D.Q., 2009. Sea level 400,000 years ago (MIS 11): analogue for present and future sea-level. *Clim. Past Discuss.* 5, 1853–1882.
- Broecker, W.S., Stocker, T.F., 2006. The Holocene CO₂ rise: anthropogenic or natural. *Eos Trans. AGU* 87 (3), 27.
- Crucifix, M., Berger, A., 2006. How long will our interglacial be? *Eos. Trans. AGU* 87 (35), 352–353.
- Dickson, A.J., Beer, C.J., Dempsey, C., Maslin, M.A., Bendle, J.A., McClymont, E.L., Pancost, R.D., 2009. Oceanic forcing of the Marine Isotope Stage 11 interglacial. *Nature Geosci.* 2, 428–433.
- Droxler, A.W., Farrell, J.W., 2000. Marine isotope stage 11 (MIS 11): new insights for a warm future. *Glob. Planet. Change* 24, 1–5.
- Dutton, A., Bard, E., Antonioli, F., Esat, T.M., Lambeck, K., McCulloch, M.T., 2009. Phasing and amplitude of sea-level and climate change during the penultimate interglacial. *Nature Geosci.* 2, 355–359.
- EPICA community members, 2004. Eight glacial cycles from an Antarctic ice core. *Nature* 429, 623–628.
- Hansen, J., Saito, M., Kharecha, P., Beerling, D., Berner, R., Masson-Delmotte, V., Pagani, M., Raymo, M., Royer, D.L., Zachos, J.C., 2008. Target atmospheric CO₂: where should humanity aim? *Open Atmos. Sci. J.* 2, 217–231.
- Hearty, P.J., Olsen, S.L., 2007. Mega-highstand or megatsunami? Discussion of McMurtry et al. (Elevated marine deposits in Bermuda record a late Quaternary megatsunami. *Sediment. Geol.* 200, 155–165. *Sediment. Geol.* 203, 307–312.
- Huybers, P., 2006. Early Pleistocene glacial cycles and the integrated summer insolation forcing. *Science* 313, 508–511.
- Jouzel, J., Masson-Delmotte, V., Cattani, O., Dreyfus, G., Falourd, S., Hoffman, G., Minster, B., Nouet, J., Barnola, J.M., Chapellaz, J., Fischer, H., Gallet, J.C., Johnsen, S., Leuenberger, M., Loulergue, L., Luthi, D., Oerter, H., Parrenin, F., Raisbeck, G., Raynaud, D., Schilt, A., Schwander, J., Selmo, E., Souchez, R., Spanhi, R., Stauffer, B., Steffensen, J.P., Stenni, B., Stocker, T.F., Tison, J.L., Werner, M., Wolff, E.W., 2007. Orbital and millennial Antarctic climate variability over the past 800,000 years. *Science* 317, 793–796.
- Kawamura, K., Parrenin, F., Lisiecki, L., Uemura, R., Vimeux, F., Severinghaus, J.P., Hutterli, M.A., Nakazawa, T., Aoki, S., Jouzel, J., Raymo, M.E., Matsumoto, K., Nakata, H., Motoyama, H., Fujita, S., Goto-Azuma, K., Fujii, Y., Watanabe, O., 2007. Northern hemisphere forcing of climatic cycles in Antarctica over the past 360,000 years. *Nature* 448, 912–917.
- Kopp, R.E., Simons, F.J., Mitrovica, J.X., Maloof, A.C., Oppenheimer, M., 2009. Probabilistic assessment of sea level during the last interglacial stage. *Nature Geosci.* 2, 863–868.
- Kutzbach, J.E., Ruddiman, W.F., Vavrus, S.J., Philippon, G., 2009. Climate model simulation of anthropogenic influence on greenhouse-induced climate change (early agriculture to modern): the role of ocean feedbacks. *Clim. Change*. doi:10.1007/s10584-009-9684-1, 31 pp.
- Laskar, J., Robutel, P., Joutel, F., Gastineau, M., Correia, A.C.M., Levrard, B., 2004. A long term numerical solution for the insolation quantities of the Earth. *Astron. Astrophys.* 428, 261–285.
- Lisiecki, L.E., Raymo, M.E., 2005. A Plio-Pleistocene stack of 57 globally distributed benthic δ¹⁸O records. *Paleoceanography* 20, PA1003. doi:10.1029/2004PA001071.
- Locke, S., Thunell, R.C., 1988. The paleoceanographic record of the last glacial-interglacial cycle in the Red-Sea and Gulf of Aden. *Palaeogeogr. Palaeoclimatol. Palaeoecol.* 64, 163–187.
- Loulergue, L., Schilt, A., Spanhi, R., Masson-Delmotte, V., Blunier, T., Lemieux, B., Barnola, J.-M., Raynaud, D., Stocker, T.F., Chappel, J., 2008. Orbital and millennial-scale features of atmospheric CH₄ over the past 800,000 years. *Nature* 453, 383–386.
- Loutre, M.F., Berger, A., 2000. Future climatic changes: are we entering an exceptionally long interglacial? *Clim. Change* 46, 61–90.
- Loutre, M.F., Berger, A., 2003. Marine Isotope Stage 11 as an analogue for the present interglacial. *Glob. Planet. Change* 36, 209–217.
- Masson-Delmotte, V., Deyfus, G., Braconnot, P., Johnsen, S., Jouzel, J., Kageyama, M., Landais, A., Loutre, M.-F., Nouet, J., Parrenin, F., Raynaud, D., Stenni, B., Tuentler, E., 2006. Past temperature reconstructions from deep ice cores: relevance for future climate change. *Clim. Past* 2, 145–165.
- McManus, J.F., Oppo, D.W., Cullen, J., 1999. A 0.5-million-year record of millennial-scale climate variability in the North Atlantic. *Science* 283, 971–975.
- McManus, J.F., Oppo, D.W., Cullen, J., Healey, S., 2003. Marine Isotope Stage 11 (MIS 11): analog for Holocene and future climate? In: Droxler, A.W., Poore, R.Z., Burckle, L.H. (Eds.), *Earth's Climate and Orbital Eccentricity: The Marine Isotope Stage 11 Question*: AGU Geophys. Monogr. Ser., vol. 137, pp. 69–85.
- Milankovitch, M.M., 1941. Canon of insolation and the ice-age problem (in German), K. Serb. Akad., Beograd (English translation, Isr. Program for Sci. Transl., Jerusalem, 1969).
- Parrenin, F., Barnola, J.-M., Beer, J., Blunier, T., Castellano, E., Chapellaz, J., Dreyfus, G., Fischer, H., Fujita, S., Jouzel, J., Kawamura, K., Lemieux-Dudon, B., Loulergue, L., Masson-Delmotte, V., Narcisi, B., Petit, J.-R., Raisbeck, G., Raynaud, D., Ruth, U., Schwander, J., Severi, M., Spanhi, R., Steffensen, J.P., Svensson, A., Udisti, R., Waelbroeck, C., Wolff, E., 2007. The EDC3 chronology for the EPICA Dome C ice core. *Clim. Past* 3, 485–497.
- Rohling, E.J., 1994. Glacial conditions in the Red Sea. *Paleoceanography* 9, 653–660.
- Rohling, E.J., Fenton, M., Jorissen, F.J., Bertrand, P., Ganssen, G., Cautlet, J.P., 1998. Magnitudes of sea-level lowstands of the past 500,000 years. *Nature* 394, 162–165.
- Rohling, E.J., Grant, K., Hemleben, Ch., Siddall, M., Hoogakker, B.A.A., Bolshaw, M., Kucera, M., 2008a. High rates of sea-level rise during the last interglacial period. *Nature Geosci.* 1, 38–42.
- Rohling, E.J., Grant, K., Hemleben, Ch., Kucera, M., Roberts, A.P., Schmeltzer, I., Schulz, H., Siccha, M., Siddall, M., Trommer, G., 2008b. New constraints on the timing and amplitude of sea level fluctuations during early to middle marine isotope stage 3. *Paleoceanography* 23, PA3219. doi:10.1029/2008PA001617.

- Rohling, E.J., Grant, K., Bolshaw, M., Roberts, A.P., Siddall, M., Hemleben, Ch., Kucera, M., 2009. Antarctic temperature and global sea level closely coupled over the past five glacial cycles. *Nature Geosci.* 2, 500–504.
- Ruddiman, W.F., 2003. The anthropocene greenhouse era began thousands of years ago. *Clim. Change* 61, 261–293.
- Ruddiman, W.F., 2005. Cold climate during the closest Stage 11 analog to recent millennia. *Quat. Sci. Rev.* 24, 1111–1121.
- Ruddiman, W.F., 2006. On “The Holocene CO₂ rise: anthropogenic or natural”. *Eos Trans. AGU* 87 (35), 352–353.
- Ruddiman, W.F., 2007. The early anthropogenic hypothesis: challenges and responses. *Rev. Geophys.* 45, RG4001. doi:10.1029/2006RG000207.
- Schmelzer, I., 1998. High-frequency event-stratigraphy and paleoceanography of the Red Sea. Ph.D. Thesis, University of Tuebingen, Tuebingen, Germany, 124 pp.
- Siccha, M., Trommer, G., Schulz, H., Hemleben, C., Kucera, M., 2009. Factors controlling the distribution of planktonic foraminifera in the Red Sea and implications for the development of transfer functions. *Mar. Micropaleontol.* 72, 146–156.
- Siddall, M., Smeed, D., Mathiessen, S., Rohling, E.J., 2002. Modelling the seasonal cycle of the exchange flow in Bab-el-Mandab (Red Sea). *Deep-Sea Res.-I* 49, 1551–1569.
- Siddall, M., Rohling, E.J., Almogi-Labin, A., Hemleben, Ch., Meischner, D., Schmeltzer, I., Smeed, D.A., 2003. Sea-level fluctuations during the last glacial cycle. *Nature* 423, 853–858.
- Siddall, M., Smeed, D.A., Hemleben, Ch., Rohling, E.J., Schmeltzer, I., Peltier, W.R., 2004. Understanding the Red Sea response to sea level. *Earth Planet. Sci. Lett.* 225, 421–434.
- Siddall, M., Bard, E., Rohling, E.J., Hemleben, Ch., 2006. Sea-level reversal during Termination II. *Geology* 34, 817–820.
- Siddall, M., Rohling, E.J., Thompson, W.G., Waelbroeck, C., 2008. Marine isotope stage 3 sea level fluctuations: data synthesis and new outlook. *Rev. Geophys.* 46, RG4003. doi:10.1029/2007RG000226.
- Siddall, M., Honisch, B., Waelbroeck, C., Huybers, P., 2009. Changes in deep Pacific temperature during the mid-Pleistocene transition and Quaternary. *Quat. Sci. Rev.* doi:10.1016/j.quascirev.2009.05.011.
- Siegenthaler, U., Stocker, T.F., Monnin, E., Lüthi, D., Schwander, J., Stauffer, B., Raynaud, D., Barnola, J.-M., Fischer, H., Mason-Delmotte, V., Jouzel, J., 2005. Stable carbon cycle–climate relationship during the Late Pleistocene. *Science* 310, 1313–1317.
- Spahni, R., Chappellaz, J., Stocker, T.F., Loulergue, L., Hausammann, G., Kawamura, K., Flückiger, J., Schwander, J., Raynaud, D., Masson-Delmotte, V., Jouzel, J., 2005. Atmospheric methane and nitrous oxide of the late Pleistocene from Antarctic ice cores. *Science* 310, 1317–1321.
- Thomas, A.L., Henderson, G.M., Deschamps, P., Yokoyama, Y., Mason, A.J., Bard, E., Hamelin, B., Durand, N., Camoin, G., 2009. Penultimate deglacial sea-level timing from Uranium/Thorium dating of Tahitian corals. *Science* 324, 1186–1189.
- Thunell, R.C., Locke, S.M., Williams, D.F., 1988. Glacio-eustatic sea-level control on Red-Sea salinity. *Nature* 334, 601–604.
- Tzedakis, P.C., 2009. The MIS 11–MIS 1 analogy, southern European vegetation, atmospheric methane and the “early anthropogenic hypothesis”. *Clim. Past Discuss* 5, 1337–1365.
- Vavrus, S., Ruddiman, W.F., Kutzbach, J.E., 2008. Climate model tests of the anthropogenic influence on greenhouse-induced climate change: the role of early human agriculture, industrialization, and vegetation feedbacks. *Quat. Sci. Rev.* 27, 1410–1425.
- Winter, A., Almogi-Labin, A., Erez, Y., Halicz, E., Luz, B., Reiss, Z., 1983. Salinity tolerance or marine organisms deduced from Red-Sea Quaternary record. *Mar. Geol.* 53, M17–M22.